Original Article

Non-alcoholic fatty liver disease is a strong predictor of carotid high-risk plaques as assessed by high-resolution magnetic resonance imaging

Tianqi Xu[1,2]^, Boning Guo[1,3]^, Sha Li[1,2]^, Shuai Zhang[2*]^, Ximing Wang[2*]^

[1]Cheeloo College of Medicine, Shandong University, Jinan, China; [2]Department of Radiology, Shandong Provincial Hospital Affiliated to Shandong First Medical University, Shandong University, Jinan, China; [3]Key Laboratory of Endocrine Glucose & Lipids Metabolism and Brain Aging, Ministry of Education, Department of Endocrinology, Shandong Provincial Hospital Affiliated to Shandong First Medical University, Jinan, China

Contributions: (I) Conception and design: T Xu, S Zhang; (II) Administrative support: X Wang; (III) Provision of study materials or patients: T Xu; (IV) Collection and assembly of data: T Xu, B Guo; (V) Data analysis and interpretation: T Xu, B Guo, S Li; (VI) Manuscript writing: All authors; (VII) Final approval of manuscript: All authors.

*These authors contributed equally to this work.

Correspondence to: Shuai Zhang, PhD; Ximing Wang, PhD. Department of Radiology, Shandong Provincial Hospital Affiliated to Shandong First Medical University, Shandong University, No. 324 Jingwu Road, Jinan 250021, China, Email: z6321106@163.com; wangxm369@sohu.com.

Background: Non-alcoholic fatty liver disease (NAFLD) is a common chronic liver disease with a high prevalence. Recent data suggest that NAFLD may be an independent risk factor for cardiovascular disease (CVD). This study aimed to investigate the association between NAFLD and carotid high-risk plaque (HRP) as assessed by high-resolution magnetic resonance imaging (MRI), and to examine the diagnostic value of NAFLD.

Methods: A total of 125 patients with carotid plaques who underwent high-resolution MRI and unenhanced abdominal computed tomography (CT) examinations were included in this retrospective study. NAFLD was defined as a liver/spleen Hounsfield unit (HU) ratio <1.0 on a non-contrast CT scan. The criteria for defining HRP were at least one of the following features: fibrous cap rupture (FCR); a large lipid-rich necrotic core (LRNC) (occupying >40% of the wall area); or intraplaque hemorrhage (IPH). Univariable and multivariable logistic regression analyses were conducted to examined the association between HRP and NAFLD. The adjusted receiver operating characteristic (aROC) curve and the adjusted area under the curve (aAUC) with the 95% confidence interval (CI) were calculated for each model.

Results: Compared with the patients without NAFLD, those with NAFLD had a higher prevalence of IPH, large LRNC, and FCR (all P<0.001). HRP was more commonly observed in the plaques of the NAFLD patients than the non-NAFLD patients (P<0.001). The multivariate analyses showed that NAFLD was an independent predictor of carotid HRP [odds ratio (OR) =12.06, 95% CI: 3.66–39.76, P<0.001]. The aROC curve analysis showed that NAFLD had an outstanding diagnostic ability (aAUC =0.95) in identifying HRP after adjusting for risk factors.

Conclusions: NAFLD is associated with carotid HRP as assessed by high-resolution MRI. CT-defined NAFLD may be a novel and robust predictor for identifying HRP.

Keywords: Non-alcoholic fatty liver disease (NAFLD); carotid plaques; high-resolution magnetic resonance imaging; unenhanced abdominal computed tomography (unenhanced abdominal CT)

^ ORCID: Tianqi Xu, 0009-0000-2533-0485; Boning Guo, 0000-0002-9655-1816; Sha Li, 0000-0002-9415-1576; Shuai Zhang, 0000-0002-9631-0411; Ximing Wang, 0000-0001-5136-8044.

Submitted Jun 30, 2024. Accepted for publication Nov 15, 2024. Published online Dec 30, 2024.
doi: 10.21037/qims-24-1326
View this article at: https://dx.doi.org/10.21037/qims-24-1326

Introduction

Non-alcoholic fatty liver disease (NAFLD) is one of the most common chronic liver diseases, and is a leading cause of liver disease-related death worldwide (1,2). NAFLD is characterized by the excessive accumulation of lipids in the liver, despite a low level of alcohol consumption, and is closely associated with a group of related metabolic disorders, including hypertension and diabetes (3). Moreover, recent research has reported an association between NAFLD and cardiovascular disease (CVD) (4). Previous studies have shown that NAFLD could be a cardiovascular risk factor, as it advances the progress of subclinical atherosclerosis or CVD (5,6). Moreover, research has shown that carotid intima-media thickness (IMT) is higher in patients with NAFLD than healthy individuals, and thus could be used as a marker for diagnosis (7).

IMT is also a marker of subclinical atherosclerosis (8). Standard carotid ultrasonography can accurately analyze morphological features and detect soft plaque. However, ultrasound resolution is limited, and ultrasonography is operator-dependent and subjective. High-resolution multi-contrast magnetic resonance imaging (MRI) can provide detailed three-dimensional (3D) anatomical images, identify carotid artery morphology, while also quantifying carotid plaque components accurately, which are associated with symptomatic presentation and may be indicative of plaque vulnerability (9). Histological correlation studies have shown that high-resolution MRI can detect characteristics of high-risk plaque (HRP) with a high degree of sensitivity and specificity (10,11).

Stroke is one of the most common causes of death worldwide (12). The main pathological characteristic of stroke is atherosclerosis, which is pathologically characterized by focal fibrosis, lipid accumulation, and atherosclerotic plaques (13). Plaques are generally classified into stable plaques and HRPs based on stability (13). Plaques that are prone to rupture, which can lead to thrombosis and severe clinical outcomes like stroke, are known as HRPs (14). Numerous studies have consistently shown a strong correlation between HRP and the incidence of cerebrovascular events; thus, the early identification of HRP could improve risk evaluation, therapeutic interventions, and prevent severe outcomes caused by HRPs (15,16). However, to date, no study has examined the association between NAFLD and carotid HRP as assessed by high-resolution MRI.

Thus, this study aimed to examined the association between NAFLD and carotid HRP as assessed by high-resolution MRI. An understanding of this relationship could be crucial in the development of targeted preventive strategies for patients with NAFLD at risk of cerebrovascular disease. Additionally, it may contribute to reducing the incidence of strokes caused by carotid atherosclerosis. We present this article in accordance with the STROBE reporting checklist (available at https://qims.amegroups.com/article/view/10.21037/qims-24-1326/rc).

Methods

Study population

The study was conducted in accordance with the Declaration of Helsinki (as revised in 2013). The study was approved by the Ethics Committee of Shandong Provincial Hospital (No. 2023-308), and the requirement of individual consent for this retrospective analysis was waived. Patient-sensitive data were protected with full confidentiality and used only for this study.

Patients with carotid plaque who underwent carotid high-resolution MRI examinations at Shandong Provincial Hospital between January 2018 and March 2023 were included in this study. To be eligible for inclusion in this study, the patients had to meet the following inclusion criteria: (I) have undergone an unenhanced abdominal computed tomography (CT) examination; and (II) have complete clinical data. Patients were excluded from the study if they met any of the following exclusion criteria: (I) had a history of alcohol intake of 30 g/d or more in men and 20 g/d in women; (II) had a history of carotid endarterectomy and stenting; (III) had cardiac thrombus, carotid occlusion, or posterior circulation symptoms; (IV) had poor-quality high-resolution MRI images; and/or (V) had an abnormal lesion at the intracranial arteries on high-resolution MRI. The study flow chart is shown in *Figure 1*.

Hypertension was defined as systolic blood pressure ≥140 mmHg or diastolic blood pressure ≥90 mmHg. Hyperlipidemia was defined as low-density lipoprotein

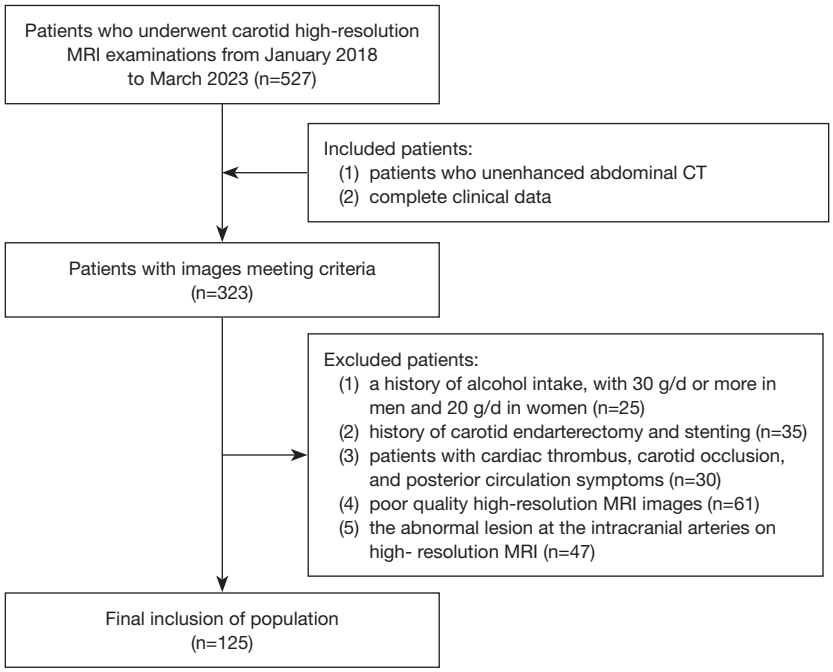

Figure 1 Flowchart of inclusion and exclusion criteria for participants. MRI, magnetic resonance imaging; CT, computed tomography.

cholesterol (LDL-C) >1.58 mmol/L, total cholesterol >2.26 mmol/L, or triglyceride (TG) >1.69 mmol/L. Diabetes was defined as a fasting serum glucose level of >6.9 mmol/L, a 2-hour post-load glucose level of >11.0 mmol/L, or the use of antidiabetic medication.

MRI

The high-resolution MRI examination was performed on a whole-body 3.0-T magnetic resonance (MR) scanner (Ingenia, Philips Healthcare, Best, The Netherlands) with a standard 64-channel head-neck coil. The scanning center was placed at the bifurcation of the carotid artery, and the patient was instructed to relax during the scanning process, breathe calmly, and minimize swallowing. The high-resolution vessel wall MRI protocol employed the following parameters: for 3D time-of-flight, fast field echo (FFE), repeat time (TR)/echo time (TE): 20 ms/3.27 ms, field of view (FOV): 230 mm × 230 mm × 70 mm, matrix: 256×256×133, slice thickness: 1 mm, number of signal averages (NSA): 1, and scan time: 2 minutes 40 seconds; for two-dimensional (2D) T1-weighed imaging, turbo spin echo (TSE), TR/TE: 1,000 ms/26 ms, FOV: 140 mm × 140 mm, matrix: 256×256, slice thickness: 2 mm (20 slices), NSA: 1, and scan time: 6 minutes 52 seconds; for 2D T2-weighted imaging, TSE, TR/TE: 2,500 ms/60 ms, FOV: 140 mm × 140 mm, matrix: 256×256, slice thickness: 2 mm (20 slices), NSA: 1, and scan time: 5 minutes 4 seconds; and for magnetization-prepared rapid acquisition gradient echo (MPRAGE), FFE, TR/TE: 8.8 ms/5.3 ms, flip angle: 15°, FOV: 140 mm × 140 mm, matrix: 256×256, slice thickness: 1 mm, inversion time: 490 milliseconds, NSA: 1, and scan time: 1 minute 23 seconds. Parallel imaging acceleration (acceleration factor: 2) was used.

CT protocol

The abdominal CT examination was performed on a third-generation dual-source CT scanner (SOMATOM Force; Siemens Healthineers, Erlangen, Germany). The CT scans were performed with a scan range from the top of the diaphragm to the inferior margin of the symphysis pubis. The abdominal CT scanning parameters were as follows: tube voltage: 120 KV; pitch: 1.0; reconstructed slice thickness: 1 mm; reconstructed slice interval: 1 mm; FOV: 350 mm × 350 mm; matrix: 512×512; spatial resolution: 0.6 mm; and rotation time: 500–600 milliseconds.

Definition of NAFLD

NAFLD was defined as a liver/spleen Hounsfield unit (HU) ratio <1.0 on a non-contrast CT scan, as previously

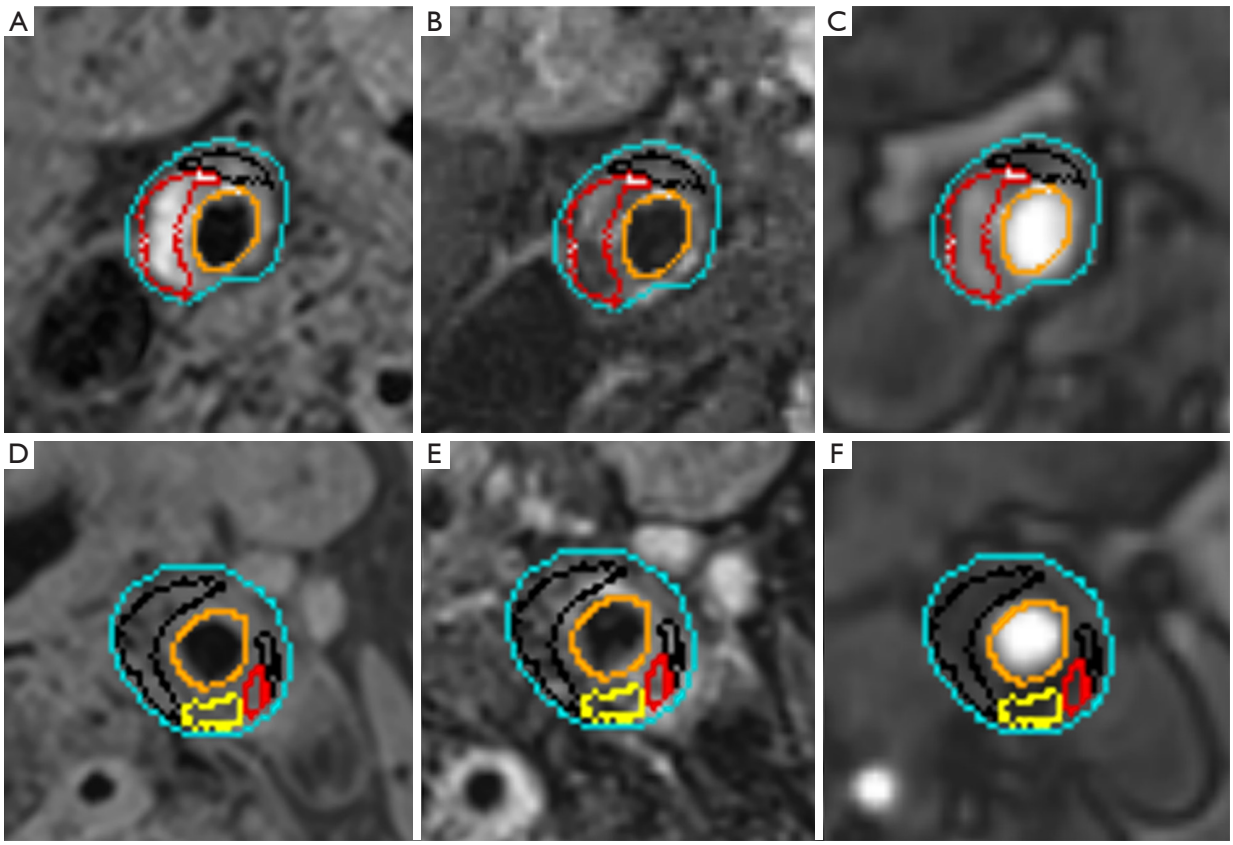

Figure 2 Carotid MRI semi-automatic segmentation of plaque composition. (A-F) The MR-PlqueView vascular plaque imaging Diagnostic System was used to delineate the plaque component regions on T1WI, T2WI, and TOF sequences. Different colors indicate different plaque components. Orange represents the lumen; blue represents the wall; red represents IPH; black represents lipids; yellow represents calcification. (A-C) Atherosclerotic plaque with IPH (outlined in red) was detected in the right carotid artery of a patient. (D-F) Atherosclerotic plaques with large LRNCs (outlined in black) were detected in the left carotid artery of a patient. MRI, magnetic resonance imaging; T1WI, T1-weighted imaging; T2WI, T2-weighted imaging; TOF, time-of-flight; IPH, intraplaque hemorrhage; LRNC, lipid-rich necrotic core.

described (17). Liver attenuation measurements were performed using previously validated methods on the right and left hepatic lobes (17). Hepatic HU was obtained by mapping three circular regions of interest with an area of at least 100 mm^2 (with a radius of approximately 5.64 mm) at an axial level. Care was taken to sample homogeneous areas representative of the parenchyma, avoiding blood vessels, bile ducts, focal lesions, focal changes of fatty liver or fatty sparing, and the surface margins.

Image analysis

Two experienced radiologists with >5 years of experience each in vascular imaging who were blinded to the patients' clinical information independently analyzed the MR images using the custom-designed software of MR-VascularView (Nanjing Jingsan Medical Science and Technology, Nanjing, China) (18). Any disagreements were resolved by a third, more experienced radiologist (with >15 years of experience in vascular imaging). The extracranial carotid artery (i.e., the common carotid artery, and the internal carotid arteries) on both sides were screened for plaque. If a carotid artery had multiple stenoses, the most severe stenosis was evaluated. The carotid lumen and wall boundaries were outlined manually at each axial location of the carotid arteries. The software automatically delineated the plaque compositions, including the lipid-rich necrotic core (LRNC), intraplaque hemorrhage (IPH), and calcification based on contrast characteristics (*Figure 2*). The morphological characteristics were measured, including the maximum wall thickness

(WT), luminal stenosis, minimal lumen area, plaque volume, and plaque burden. The luminal stenosis was measured using the North American Symptomatic Carotid Endarterectomy Trial criteria for extracranial carotid arteries (19). Stenosis, the minimal luminal area, plaque volume, and plaque burden were calculated automatically using MR-VascularView. The vessel area was calculated as the lumen area plus the vessel wall area. Plaque burden was measured on the maximal stenosis site as follows:

Plaque burden = (1 – lumen area/vessel area) × 100%

The criteria for defining HRP were fibrous cap rupture (FCR), a large LRNC (occupying > 40% of the wall area), or IPH, which was assessed using the American Heart Association (AHA) plaque typing method (20). Radiologist A (with >5 years of experience in plaque imaging) completed segmentation of plaque compositions for all patients. Another Radiologist B (with >5 years of experience in plaque imaging) re-segmented 40 randomly selected datasets to calculate the inter-observer-agreement. Three months after the first round of segmentation, Radiologist A re-segmented and feature-analyzed the 40 randomly selected datasets to calculate the intra-observer-agreement. This subset of patients was used to calculate the intra-class correlation coefficients (ICCs).

Statistical analysis

The Shapiro-Wilk normality test was used to verify the normality of the data distribution. The continuous variables are described as the mean ± standard deviation (SD), while the categorical variables are presented as the percentage. The clinical characteristics and carotid plaque characteristics were compared between the patients with NAFLD and without NAFLD using a *t*-test and chi-square test. Univariate and multivariable logistic regression analyses with generalized estimating equation correction was used to calculate the odds ratio (OR) and corresponding 95% confidence interval (CI) of NAFLD in detecting the presence of carotid HRP. The adjusted receiver operating characteristic (aROC) curve, adjusted area under the curve (aAUC) with the 95% CI: sensitivity, and specificity were calculated for each model. Intra- and inter-reader agreement in measuring features was calculated using the ICC. A P value <0.05 represented statistical significance. All statistical analyses were performed using SPSS 22.0 (IBM, Chicago, IL, USA) and R statistical software (version 4.3.2, R Foundation for Statistical Computing).

Results

Clinical characteristics

A total of 323 patients who underwent carotid high-resolution MRI and abdominal CT examinations were identified for inclusion in the study. However, among these patients, 25 had an alcohol intake ≥30 g/day in men and 20 g/day in women, 35 had a history of carotid endarterectomy and stenting, 30 had a history of cardiac thrombus, carotid occlusion, and posterior circulation symptoms, 61 had poor-quality images, and 47 had an abnormal lesion at the intracranial arteries on high-resolution MRI, and were thus excluded from the study. Ultimately, 125 patients were included in the study (age: 58.1±12.1 years; 102 males). All the included patients with carotid plaques were divided into two groups: the NAFLD group (which comprised 54 patients) and the non-NAFLD group (which comprised 71 patients). Compared with the patients in the non-NAFLD group, those in the NAFLD group were more likely to have hyperlipidemia (P=0.034), but no other significant differences were found between the two groups in terms of the other factors (all P>0.05) (*Table 1*).

Comparison of MRI characteristics between patients with and without NAFLD

Compared to the patients without NAFLD, those with NAFLD had a higher prevalence of HRP (83.3% versus 15.5%, P<0.001) (*Table 2* and *Figure 3*). The prevalence of various carotid plaque components was evaluated in patients with NAFLD. Compared to the patients without NAFLD, those with NAFLD had a higher prevalence of IPH (81.5% versus 15.5%, P<0.001), large LRNC (77.8% versus 12.7%, P<0.001), FCR (44.4% versus 7.0%, P<0.001), and calcification (94.4% versus 73.2%, P=0.002) (*Table 2* and *Figure 4*). Notably, HRP was more frequently found in the plaques of the NAFLD patients than the non-NAFLD patients (83.3% versus 15.5%, P<0.001). Additionally, compared to the plaques of patients in the non-NAFLD group, the plaques of the patients in the NAFLD group had a significantly greater maximum WT (4.6±0.9 versus 3.7±0.9 mm, P<0.001), severer stenosis (47.7%±9.7% versus 35.4%±13.4%, P<0.001), a greater plaque volume (1,861.2±1,222.8 versus 1,351.4±1,059.7 mm^3, P=0.014), and a greater plaque burden (66.7±9.3 versus 60.8±10.8, P=0.002). There were no significant differences in the prevalence of the minimal lumen area between the two

Table 1 Clinical characteristics

Variables	Total (n=125)	NAFLD group (n=54)	Non-NAFLD group (n=71)	P
Age, years	58.1±12.1	59.2±11.2	57.2±12.7	0.360
Male	102 (81.6)	48 (88.9)	54 (76.1)	0.067
Hypertension	62 (49.6)	30 (55.6)	32 (45.1)	0.245
Hyperlipidemia	28 (22.4)	17 (31.5)	11 (15.5)	0.034
Smoking	52 (41.6)	26 (48.1)	26 (36.6)	0.195
Medication in use				
Antihypertension use	36 (28.8)	17 (31.5)	19 (26.8)	0.564
Statin use	19 (15.2)	12 (22.2)	7 (9.9)	0.057
Laboratory findings				
AST, U/L	23.2±7.8	24.0±8.8	22.6±6.9	0.302
ALT, U/L	27.1±16.5	39.8±19.9	25.1±13.2	0.110
GGT, U/L	35.0±23.1	34.7±17.2	35.2±26.8	0.891
HDL-C, mmol/L	1.2±0.3	1.1±0.3	1.2±0.4	0.141
LDL-C, mmol/L	2.4±0.8	2.4±0.9	2.4±0.8	0.688
TG, mmol/L	1.4±1.0	1.5±1.1	1.4±0.9	0.513
Uric acid, μmol/L	330.9±78.3	346.3±74.8	319.3±79.3	0.056

Data are presented as the mean ± standard deviation, or number (%). NAFLD, non-alcoholic fatty liver disease; AST, aspartate aminotransferase; ALT, alanine transaminase; GGT, gamma-glutamyl transferase; HDL-C, high-density lipoprotein cholesterol; LDL-C, low-density lipoprotein cholesterol; TG, triglyceride.

Table 2 Comparison of plaque characteristics between NAFLD and non-NAFLD groups

Variables	Total (n=125)	NAFLD group (n=54)	Non-NAFLD group (n=71)	P
Presence of plaque components				
IPH	55 (44.0)	44 (81.5)	11 (15.5)	<0.001
Large LRNC	51 (40.8)	42 (77.8)	9 (12.7)	<0.001
FCR	29 (23.2)	24 (44.4)	5 (7.0)	<0.001
Calcification	103 (82.4)	51 (94.4)	52 (73.2)	0.002
Presence of HRP	56 (44.8)	45 (83.3)	11 (15.5)	<0.001
Maximum wall thickness, mm	4.1±1.0	4.6±0.9	3.7±0.9	<0.001
Stenosis, %	40.5±13.3	47.7±9.7	35.4±13.4	<0.001
Minimal lumen area, mm^2	25.6±24.3	27.5±26.4	24.2±22.8	0.466
Plaque volume, mm^3	1,571.6±1,156.4	1,861.2±1,222.8	1,351.4±1,059.7	0.014
Plaque burden (%)	63.3±10.6	66.7±9.3	60.8±10.8	0.002

Data are presented as the mean ± standard deviation, or number (%). NAFLD, non-alcoholic fatty liver disease; IPH, intraplaque hemorrhage; LRNC, lipid-rich necrotic core; FCR, fibrous cap rupture; HRP, high-risk plaque.

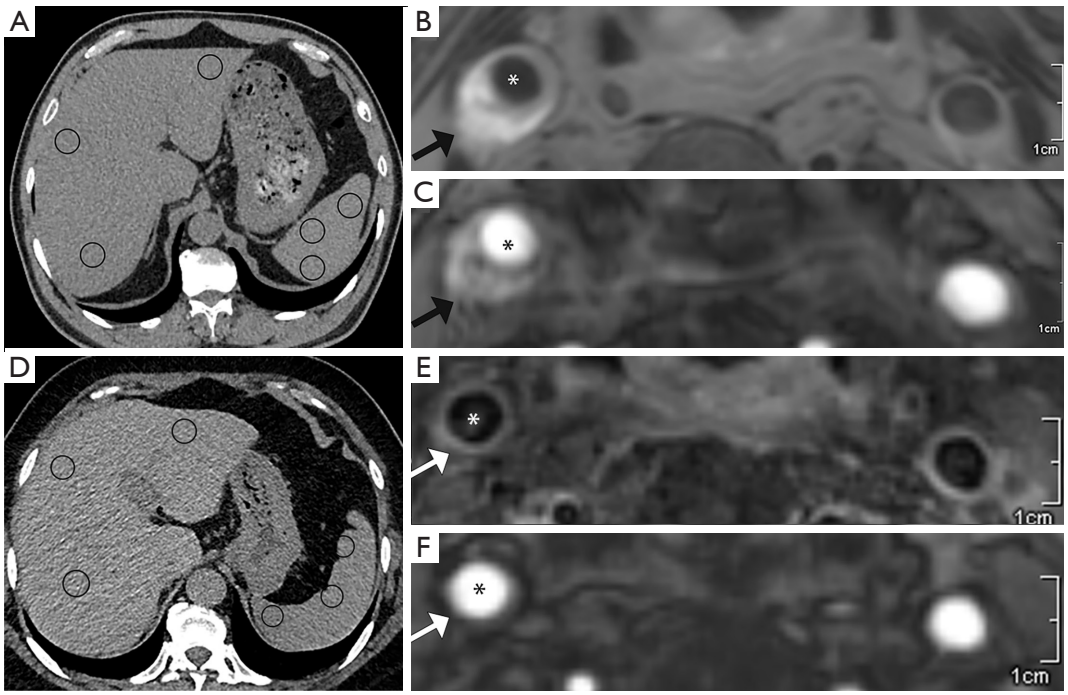

Figure 3 Analysis of carotid plaques in patients with and without NAFLD. (A) Diffuse fat accumulation was observed in a liver in an unenhanced CT image with a liver/spleen ratio of 0.81; (B) axial T1WI clearly showed the hypersignal of IPH (black arrow); (C) axial 2D-TOF showed IPH with a hypersignal (black arrow). (D) Diffuse fat accumulation was observed in a liver in an unenhanced CT image with a liver/spleen ratio of 1.12; (E) axial T1WI clearly showed the absence of IPH (white arrow); (F) axial 2D-TOF showed the absence of IPH (white arrow). (○) indicates the measurements of mean CT values of the liver/spleen; (*) indicates the lumen of the carotid artery. NAFLD, non-alcoholic fatty liver disease; CT, computed tomography; T1WI, T1-weighted imaging; IPH, intraplaque hemorrhage; TOF, time-of-flight.

groups (P>0.05).

Logistic regression analysis

As *Table 3* shows, the univariate logistic regression analysis identified the presence of NAFLD (OR =27.27; 95% CI: 10.42–71.37, P<0.001), maximum WT (OR =4.01; 95% CI: 2.37–6.80, P<0.001), luminal stenosis (OR =1.13; 95% CI: 1.08–1.18, P<0.001), plaque volume (OR =1.00; 95% CI: 1.00–1.00, P<0.001), plaque burden (OR =1.07; 95% CI: 1.03–1.11, P=0.001), statin use (OR =4.27; 95% CI: 1.43–12.73, P=0.009), and uric acid (OR =1.01; 95% CI: 1.00–1.01, P=0.029) as significant variables, which were subsequently entered into the multivariate analysis (*Table 3*). The multivariable logistic regression analysis further revealed that NAFLD (OR =12.06, 95% CI: 3.66–39.76, P<0.001), maximum WT (OR =2.28, 95% CI: 1.08–4.82, P=0.031), luminal stenosis (OR =1.10; 95% CI: 1.03–1.17, P=0.003), and statin use (OR =5.72; 95% CI: 1.02–32.03, P=0.047) were independent predictors of carotid HRP (*Table 3*).

The intra- and inter-observer agreement results for quantifying carotid features are set out in *Table 4*. The results of the aROC curve analysis of whether of NAFLD can predict carotid HRP on MRI are shown in *Figure 5*. The aAUCs of the four models were excellent: 0.92 (95% CI: 0.87–0.96) for the clinical risk factor model (sensitivity 85.71%, specificity 85.51%); 0.88 (95% CI: 0.82–0.95) for the laboratory findings model (sensitivity 80.36%, specificity 89.86%); 0.94 (95% CI: 0.90–0.98) for the plaque characteristics model (sensitivity 83.93%, specificity 91.30%); and 0.95 (95% CI: 0.91–0.98) for the model that included the factors with a P value <0.05 from the univariable analysis (sensitivity 89.29%, specificity 86.96%).

Discussion

Previous studies have reported an association between

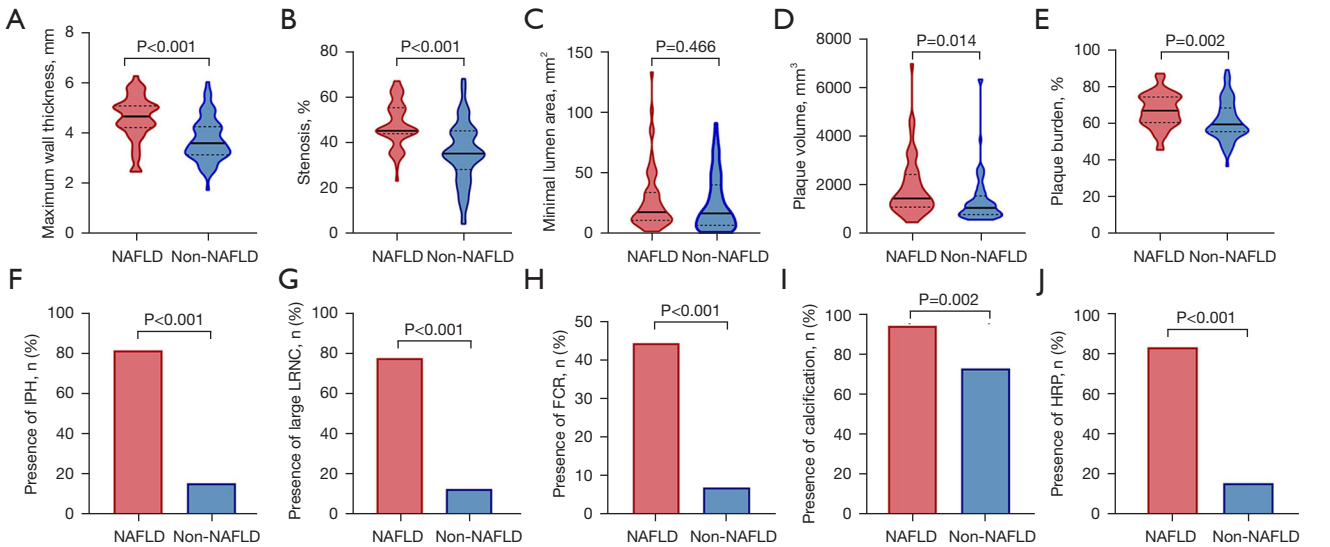

Figure 4 Comparison of MRI characteristics according to the presence of NAFLD. (A) Maximum wall thickness; (B) lumen stenosis; (C) minimal lumen area; (D) plaque volume; (E) plaque burden; (F) presence of IPH; (G) presence of large LRNC; (H) presence of FCR; (I) presence of calcification; (J) presence of HRP. Compared with the plaques in the non-NAFLD group, the plaques in the NAFLD group showed significantly greater maximum wall thickness, severer stenosis, a greater plaque volume, and a greater plaque burden (all P<0.05). Compared with the patients without NAFLD, those with NAFLD had higher prevalence of IPH, a large LRNC, FCR, calcification, and HRP (all P<0.05). NAFLD, non-alcoholic fatty liver disease; MRI, magnetic resonance imaging; IPH, intraplaque hemorrhage; LRNC, lipid-rich necrotic core; FCR, fibrous cap rupture; HRP, high-risk plaque.

NAFLD, subclinical myocardial dysfunction, coronary circulation, carotid atherosclerosis, and increased cerebrovascular risks (21-23). The present study found a strong correlation between NAFLD and carotid HRP as assessed by high-resolution MRI. Notably, MRI is a non-invasive and radiation-free technique that can be used to identify various components of carotid plaques. Our findings suggest that NAFLD is a valuable predictor of HRP. The early screening of carotid HRP in patients with NAFLD may help to identify individuals at increased risk of cerebrovascular events and thus facilitate timely risk management. Moreover, exploring the differences in carotid plaques between patients with and without NAFLD may help elucidate the potential mechanisms of atherosclerotic plaque initiation and development, and refine the stratification of stroke risk.

The stenosis rate is the primary indicator of ischemic stroke risk; however, plaque components are becoming increasingly recognized as important in assessing stroke risk, as shown by the current study. In this study, we performed a more extensive evaluation of carotid HRP. We found that patients with NAFLD were more likely to have carotid HRP with IPH, a large LRNC, or FCR than those without NAFLD. Recent studies have shown that IPH, an emerging marker of plaque instability, is an important risk factor for stroke (24,25). Moreover, the size of the LRNC in carotid plaques is believed to be a predictive factor for plaque rupture, and can be used to differentiate between symptomatic and asymptomatic patients (26). Additionally, fibrous cap status is an important characteristic of carotid plaques (27). Carotid plaques with FCR are more likely to be associated with a recent transient ischemic attack or stroke (28). Further, carotid plaque with a core lipid pool that occupies >40% of the wall area should be classified as unstable (29).

Previous studies have shown that perivascular adipose tissue is a potential indicator of vulnerable atherosclerotic plaques, and can be used to distinguish between different stages of carotid atherosclerotic disease (30,31). Among the patients with carotid plaque included in this study, we found that NAFLD was associated with carotid HRP. This association persisted after adjusting for clinical risk factors, laboratory findings, plaque characteristics, and factors with P values <0.05. The aROC curves showed that NAFLD had a high predictive value for carotid HRP. Several studies have reported that NAFLD is associated with an increased

Table 3 Univariate and multivariate logistic regression analyses for identifying HRP on MRI

Parameter	Plaques of participants with and without HRP			
	Univariate regression		Multivariate regression	
	OR (95% CI)	P	OR (95% CI)	P
NAFLD	27.27 (10.42–71.37)	<0.001	12.06 (3.66–39.76)	<0.001
Maximum wall thickness, mm	4.01 (2.37–6.80)	<0.001	2.28 (1.08–4.82)	0.031
Stenosis, %	1.13 (1.08–1.18)	<0.001	1.10 (1.03–1.17)	0.003
Minimal lumen area, mm^2	1.00 (0.98–1.01)	0.697	–	–
Plaque volume, mm^3	1.00 (1.00–1.00)	<0.001	1.00 (1.00–1.00)	0.107
Plaque burden	1.07 (1.03–1.11)	0.001	1.01 (0.95 - 1.07)	0.839
Age, years	1.03 (0.99–1.06)	0.118	–	–
Male	2.72 (0.99–7.47)	0.051	–	–
Hypertension	1.03 (0.51–2.08)	0.936	–	–
Hyperlipidemia	2.30 (0.97–5.43)	0.058	–	–
Smoking	1.64 (0.80–3.36)	0.178	–	–
Medication in use			–	–
Antihypertension use	0.98 (0.45–2.14)	0.959	–	–
Statin use	4.27 (1.43–12.73)	0.009	5.72 (1.02–32.03)	0.047
Laboratory findings				
AST, U/L	1.01 (0.97–1.06)	0.574	–	–
ALT, U/L	1.01 (0.99–1.04)	0.230	–	–
GGT, U/L	0.99 (0.98–1.01)	0.429	–	–
HDL-C, mmol/L	0.40 (0.12–1.30)	0.127	–	–
LDL-C, mmol/L	0.96 (0.63–1.46)	0.840	–	–
TG, mmol/L	1.04 (0.72–1.50)	0.855	–	–
Uric acid, μmol/L	1.01 (1.00–1.01)	0.029	1.00 (0.99–1.01)	0.796

HRP, high-risk plaque; MRI, magnetic resonance imaging; OR, odds ratio; CI, confidence interval; NAFLD, non-alcoholic fatty liver disease; AST, aspartate aminotransferase; ALT, alanine transaminase; GGT, gamma-glutamyl transferase; HDL-C, high-density lipoprotein cholesterol; LDL-C, low-density lipoprotein cholesterol; TG, triglyceride.

Table 4 Intra- and inter-class correlation coefficients of features

Variables	Intra-class correlation coefficients (95% CI)	Inter-class correlation coefficients (95% CI)
Stenosis	0.946 (0.900, 0.971)	0.914 (0.843, 0.953)
Minimal luminal area	0.962 (0.928, 0.979)	0.887 (0.797, 0.939)
Plaque volume	0.915 (0.845, 0.954)	0.872 (0.771, 0.930)
Plaque burden	0.848 (0.732, 0.917)	0.803 (0.658, 0.891)
Maximum wall thickness	0.935 (0.880, 0.965)	0.868 (0.763, 0.928)

CI, confidence interval.

incidence of CVD. In one prospective study, the severity of NAFLD was found to be associated with a higher risk of future ischemic stroke events (32). In a meta-analysis of 16 unique studies with 34,043 adult individuals, the patients with NAFLD had a higher risk of fatal or non-fatal CVD events than those without NAFLD over a median period of 6.9 years, which is consistent with the conclusions of the present study (33).

In this study, the patients with NAFLD were more

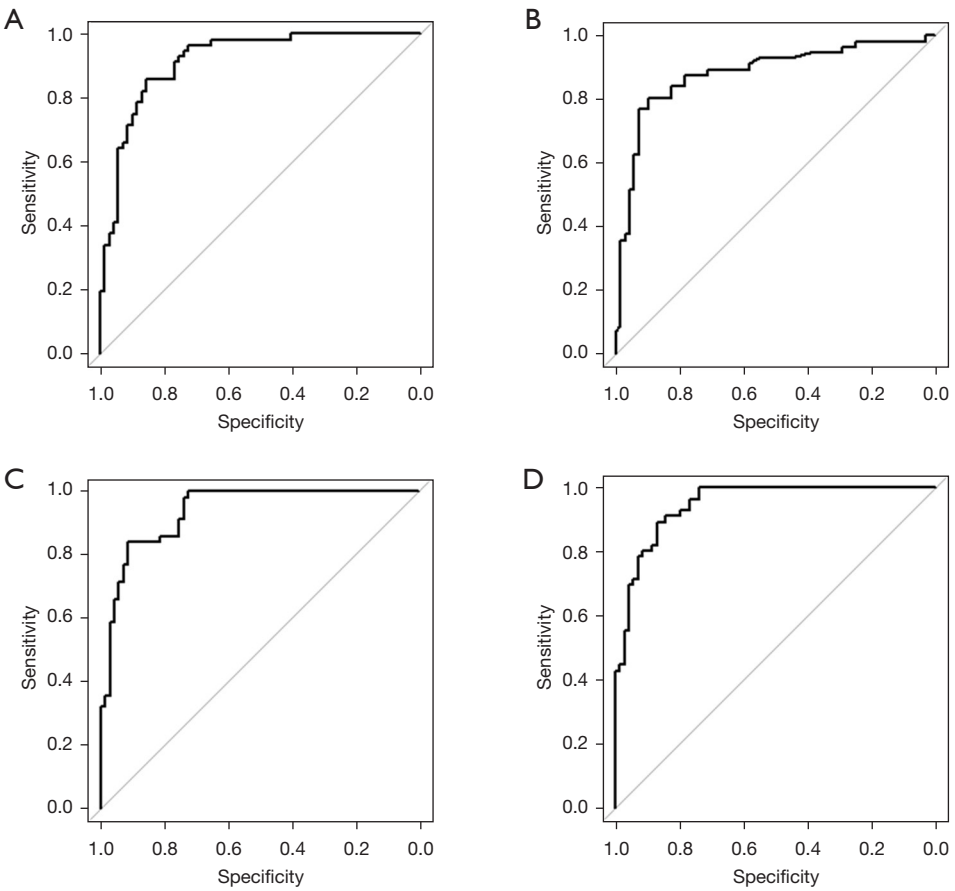

Figure 5 aROC curves of the four NAFLD models for predicting carotid HRP on MRI. (A) aAUC was adjusted for age, sex (male), hypertension, hyperlipidemia, a family history of CHD, diabetes, smoking, stroke, antihypertension use, statin use, anticoagulant use, and antiplatelet use. (B) aAUC was adjusted for AST, ALT, GGT, HDL-C, LDL-C, TG, and uric acid. (C) aAUC was adjusted for maximum WT, stenosis, maximum lumen area, plaque volume, and plaque burden. (D) aAUC was adjusted for stroke, statin use, uric acid, maximum WT, stenosis, plaque volume, and plaque burden. aROC, adjusted receiver operating characteristic curve; NAFLD non-alcoholic fatty liver disease; HRP, high-risk plaque; MRI, magnetic resonance imaging; aAUC, adjusted area under the curve; CHD, coronary heart disease; AST, aspartate aminotransferase; ALT, alanine transaminase; GGT, gamma-glutamyl transferase; HDL-C, high-density lipoprotein cholesterol; LDL-C, low-density lipoprotein cholesterol; TG, triglyceride; WT, wall thickness.

likely to have hyperlipidemia than the patients without NAFLD. Some studies have suggested that NAFLD is a hepatic manifestation of metabolic syndrome, and is often accompanied by hyperlipidemia and obesity (34,35). Elevated serum alanine transaminase (ALT), aspartate aminotransferase (AST), gamma-glutamyl transferase (GGT), total cholesterol, and uric acid levels have been shown to be strongly related to CVD, liver diseases like NAFLD, and metabolic syndrome (36,37). Lipid-lowering drugs, such as statins, have been shown to have a certain therapeutic effect in managing hyperlipidemia and lowering the risk of cerebrovascular disease in these patients (38). However, in this study, the patients who had received baseline statin therapy had a significantly higher rate of HRP than those who had not received statin therapy. However, this result should be interpreted cautiously, as information on the duration of statin therapy was not recorded.

Various theories have been proposed as to the common mechanism underlying the progression of NAFLD and atherosclerosis. Oxidative stress and subclinical inflammation, which play a major role in the progression and pathology of NAFLD, induce endothelial dysfunction, which may lead to systemic vascular sclerosis (39). Levine

et al. found that the severity of NAFLD increases the plasminogen activator inhibitor 1 levels, thereby increasing the risk of atherosclerosis progression (40). Additionally, NAFLD may be an active mediator that contributes directly to the progression of atherosclerosis (41). However, it is still unclear whether NAFLD is a marker of cardiometabolic risk, or whether NAFLD directly affects atherogenesis and atherothrombotic risk.

The present study had some limitations. First, this was a cross-sectional study; thus, prospective studies are needed to investigate the association between NAFLD and the progression of carotid HRP. Second, NAFLD was defined at CT and was not confirmed by liver biopsy. However, performing a liver biopsy in an epidemiologic study would be unacceptable. Third, we only used high-resolution MRI to evaluate carotid plaque features. Relevant pathological studies are needed to confirm our findings in the future.

Conclusions

This study showed that NAFLD is associated with carotid HRP as assessed by high-resolution MRI. Our findings suggest that NAFLD had a high diagnostic value for carotid HRP. Our findings could provide valuable guidance in clinical practice and future research in this important area of cardiovascular risk management in NAFLD patients. Thus, consideration should be given to incorporating NAFLD into future guidelines for cerebrovascular disease prevention, and including it among the potential risk factors for cerebrovascular damage.

Acknowledgments

Funding: This study was supported by the National Natural Science Foundation of China (No. 82271993).

Footnote

Reporting Checklist: The authors have completed the STROBE reporting checklist. Available at https://qims.amegroups.com/article/view/10.21037/qims-24-1326/rc

Conflicts of Interest: All authors have completed the ICMJE uniform disclosure form (available at https://qims.amegroups.com/article/view/10.21037/qims-24-1326/coif). The authors have no conflicts of interest to declare.

Ethical Statement: The authors are accountable for all aspects of the work in ensuring that questions related to the accuracy or integrity of any part of the work have been appropriately investigated and resolved. The study was conducted in accordance with the Declaration of Helsinki (as revised in 2013). The study was approved by the Ethics Committee of Shandong Provincial Hospital (No. 2023-308), and the requirement of individual consent for this retrospective analysis was waived.

References

1. Pouwels S, Sakran N, Graham Y, et al. Non-alcoholic fatty liver disease (NAFLD): a review of pathophysiology, clinical management and effects of weight loss. BMC Endocr Disord 2022;22:63.
2. Teng ML, Ng CH, Huang DQ, et al. Global incidence and prevalence of nonalcoholic fatty liver disease. Clin Mol Hepatol 2023;29:S32-42.
3. Adams LA, Anstee QM, Tilg H, et al. Non-alcoholic fatty liver disease and its relationship with cardiovascular disease and other extrahepatic diseases. Gut 2017;66:1138-53.
4. Bali AD, Rosenzveig A, Frishman WH, et al. Nonalcoholic Fatty Liver Disease and Cardiovascular Disease: Causation or Association. Cardiol Rev 2024;32:453-62.
5. Martins E, Oliveira A. NAFLD and cardiovascular disease. Porto Biomed J 2018;3:e2.
6. Koulaouzidis G, Charisopoulou D, Kukla M, et al. Association of non-alcoholic fatty liver disease with coronary artery calcification progression: a systematic review and meta-analysis. Prz Gastroenterol 2021;16:196-206.
7. Rampally V, Biri SK, Nair IK, et al. Determination of association between nonalcoholic fatty liver disease and carotid artery atherosclerosis among nondiabetic individuals. J Family Med Prim Care 2020;9:1182-6.
8. Gierach M, Junik R. The Level of Intima-Media Thickness in Patients with Metabolic Syndrome in Poland Depending on the Prevalence of Type 2 Diabetes. Biomedicines 2023;11:1510.

9. Watase H, Sun J, Hippe DS, et al. Carotid Artery Remodeling Is Segment Specific: An In Vivo Study by Vessel Wall Magnetic Resonance Imaging. Arterioscler Thromb Vasc Biol 2018;38:927-34.
10. Yuan C, Mitsumori LM, Ferguson MS, et al. In vivo accuracy of multispectral magnetic resonance imaging for identifying lipid-rich necrotic cores and intraplaque hemorrhage in advanced human carotid plaques. Circulation 2001;104:2051-6.
11. Fabiano S, Mancino S, Stefanini M, et al. High-resolution multicontrast-weighted MR imaging from human carotid endarterectomy specimens to assess carotid plaque components. Eur Radiol 2008;18:2912-21.
12. Khandelwal P, Yavagal DR, Sacco RL. Acute Ischemic Stroke Intervention. J Am Coll Cardiol 2016;67:2631-44.
13. Jiao Y, Qin Y, Zhang Z, et al. Early identification of carotid vulnerable plaque in asymptomatic patients. BMC Cardiovasc Disord 2020;20:429.
14. Huang R, Cao Y, Li H, et al. miR-532-3p-CSF2RA Axis as a Key Regulator of Vulnerable Atherosclerotic Plaque Formation. Can J Cardiol 2020;36:1782-94.
15. Liu XS, Zhao HL, Cao Y, et al. Comparison of carotid atherosclerotic plaque characteristics by high-resolution black-blood MR imaging between patients with first-time and recurrent acute ischemic stroke. AJNR Am J Neuroradiol 2012;33:1257-61.
16. Wang Y, Wang T, Luo Y, et al. Identification Markers of Carotid Vulnerable Plaques: An Update. Biomolecules 2022;12:1192.
17. Zeb I, Li D, Nasir K, et al. Computed tomography scans in the evaluation of fatty liver disease in a population based study: the multi-ethnic study of atherosclerosis. Acad Radiol 2012;19:811-8.
18. Zhang R, Zhang Q, Ji A, et al. Prediction of new cerebral ischemic lesion after carotid artery stenting: a high-resolution vessel wall MRI-based radiomics analysis. Eur Radiol 2023;33:4115-26.
19. Ferguson GG, Eliasziw M, Barr HW, et al. The North American Symptomatic Carotid Endarterectomy Trial : surgical results in 1415 patients. Stroke 1999;30:1751-8.
20. Xu D, Hippe DS, Underhill HR, et al. Prediction of high-risk plaque development and plaque progression with the carotid atherosclerosis score. JACC Cardiovasc Imaging 2014;7:366-73.
21. Tang ASP, Chan KE, Quek J, et al. Non-alcoholic fatty liver disease increases risk of carotid atherosclerosis and ischemic stroke: An updated meta-analysis with 135,602 individuals. Clin Mol Hepatol 2022;28:483-96.
22. Sonaglioni A, Cerini F, Nicolosi GL, et al. Left ventricular strain predicts subclinical atherosclerosis in nonadvanced nonalcoholic fatty liver disease patients. Eur J Gastroenterol Hepatol 2022;34:707-16.
23. De Filippo O, Di Pietro G, Nebiolo M, et al. Increased prevalence of high-risk coronary plaques in metabolic dysfunction associated steatotic liver disease patients: A meta-analysis. Eur J Clin Invest 2024;54:e14188.
24. Przybyszewski EM, Targher G, Roden M, et al. Nonalcoholic Fatty Liver Disease and Cardiovascular Disease. Clin Liver Dis (Hoboken) 2021;17:19-22.
25. Xiong Z, Peng K, Song S, et al. Cerebral Intraparenchymal Hemorrhage Changes Patients' Gut Bacteria Composition and Function. Front Cell Infect Microbiol 2022;12:829491.
26. Xia J, Yin A, Li Z, et al. Quantitative Analysis of Lipid-Rich Necrotic Core in Carotid Atherosclerotic Plaques by In Vivo Magnetic Resonance Imaging and Clinical Outcomes. Med Sci Monit 2017;23:2745-50.
27. Sun J, Zhao XQ, Balu N, et al. Carotid Plaque Lipid Content and Fibrous Cap Status Predict Systemic CV Outcomes: The MRI Substudy in AIM-HIGH. JACC Cardiovasc Imaging 2017;10:241-9.
28. Watanabe Y, Nagayama M. MR plaque imaging of the carotid artery. Neuroradiology 2010;52:253-74.
29. Bentzon JF, Otsuka F, Virmani R, et al. Mechanisms of plaque formation and rupture. Circ Res 2014;114:1852-66.
30. Yu S, Huo R, Qiao H, et al. Carotid artery perivascular adipose tissue on magnetic resonance imaging: a potential indicator for carotid vulnerable atherosclerotic plaque. Quant Imaging Med Surg 2023;13:7695-705.
31. Liu X, Wu F, Jia X, et al. Pericarotid adipose tissue computed tomography attenuation distinguishes different stages of carotid atherosclerotic disease: a cross-sectional study. Quant Imaging Med Surg 2023;13:8247-58.
32. Lu ZY, Shao Z, Li YL, et al. Prevalence of and risk factors for non-alcoholic fatty liver disease in a Chinese population: An 8-year follow-up study. World J Gastroenterol 2016;22:3663-9.
33. Targher G, Byrne CD, Lonardo A, et al. Non-alcoholic fatty liver disease and risk of incident cardiovascular disease: A meta-analysis. J Hepatol 2016;65:589-600.
34. Zhang QQ, Lu LG. Nonalcoholic Fatty Liver Disease: Dyslipidemia, Risk for Cardiovascular Complications, and Treatment Strategy. J Clin Transl Hepatol 2015;3:78-84.
35. Srivastava A, Kaze AD, McMullan CJ, et al. Uric Acid and the Risks of Kidney Failure and Death in Individuals With CKD. Am J Kidney Dis 2018;71:362-70.
36. Al Rifai M, Silverman MG, Nasir K, et al. The association

of nonalcoholic fatty liver disease, obesity, and metabolic syndrome, with systemic inflammation and subclinical atherosclerosis: the Multi-Ethnic Study of Atherosclerosis (MESA). Atherosclerosis 2015;239:629-33.
37. Martin A, Lang S, Goeser T, et al. Management of Dyslipidemia in Patients with Non-Alcoholic Fatty Liver Disease. Curr Atheroscler Rep 2022;24:533-46.
38. Francque SMA, Dirinck E. NAFLD prevalence and severity in overweight and obese populations. Lancet Gastroenterol Hepatol 2023;8:2-3.
39. Monserrat-Mesquida M, Quetglas-Llabrés M, Abbate M, et al. Oxidative Stress and Pro-Inflammatory Status in Patients with Non-Alcoholic Fatty Liver Disease. Antioxidants (Basel) 2020;9:759.
40. Levine JA, Oleaga C, Eren M, et al. Role of PAI-1 in hepatic steatosis and dyslipidemia. Sci Rep 2021;11:430.
41. Fotbolcu H, Zorlu E. Nonalcoholic fatty liver disease as a multi-systemic disease. World J Gastroenterol 2016;22:4079-90.

Cite this article as: Xu T, Guo B, Li S, Zhang S, Wang X. Non-alcoholic fatty liver disease is a strong predictor of carotid high-risk plaques as assessed by high-resolution magnetic resonance imaging. Quant Imaging Med Surg 2025;15(1):898-910. doi: 10.21037/qims-24-1326